Simulation of Electromagnetic Wave Propagation in a Magnetospheric Plasma*)

Takahiro MORI[1)], Masaki NISHIURA[1,2)], Zensho YOSHIDA[1)], Naoki KENMOCHI[1)], Shotaro KATSURA[1)], Kaori NAKAMURA[1)], Yuuki YOKOTA[1)], Toru I. TSUJIMURA[2)] and Shin KUBO[2)]

[1)]*Graduate School of Frontier Sciences, The University of Tokyo, Kashiwa, Chiba 277-8561, Japan*
[2)]*National Institute for Fusion Science, Toki 509-5292, Japan*

(Received 8 January 2019 / Accepted 8 May 2019)

The Ring Trap 1 (RT-1) device creates a laboratory magnetosphere, that is motivated by the Jovian magnetosphere, which contains self-organized, high-beta plasmas. In the RT-1 plasmas, the density limit for 8.2 GHz electron cyclotron heating (ECH) occurs at the electron densities 8.0×10^{17} m^{-3} and for 2.45 GHz ECH, 1.6×10^{17} m^{-3}. We have used full-wave simulations to study the propagation and absorption of electromagnetic waves in the RT-1 plasmas in an effort to understand the observed density limits as well as the over-dense state in which the actual density exceeds the cutoff density of the magnetospheric plasma. The simulation results cannot explain the experimentally observed over-dense states and density limits in the view of the power absorption. We discuss possible reasons for the gap between the experiments and the simulation results.

Keywords: magnetospheric plasma, ECH, electron cyclotron wave, electric field, over dense plasma, electromagnetic wave propagation

DOI: 10.1585/pfr.14.3401134

1. Introduction

A dipole field is a basic structure in nature for plasma confinement, and it is an appropriate subject of study for extracting universal physical principles. The Ring Trap 1 (RT-1) device is motivated by the Jovian magnetosphere, and it enables us to study both magnetospheric plasma physics and advanced fusion. The RT-1 device has previously demonstrated plasma confinement in a dipole field using a levitated superconducting ring magnet [1], which produces the dipole fields necessary for plasma confinement. The plasmas are produced by electron cyclotron (EC) heating using either or both 2.45 GHz and 8.2 GHz electromagnetic (EM) waves. The plasma so produced has a peaked density profile, which is a self-organized structure that is also observed in naturally formed planetary magnetospheres. The measured density in the RT-1 device is shown below in Fig. 2. The aim of the present work is to extend the operation regime of the device.

For 8.2 GHz EM wave, we found that the line averaged electron density is limited to the range below the cutoff density. However, we found experimentally that a 2.45 GHz EM wave usually overcomes the 2.45 GHz cutoff density, even when the same interferometer chord is used to measure the density. Understanding the propagation and absorption of the EM waves is thus essential to distill the underlying physics from the apparent density limits in the 8.2 and 2.45 GHz EC heating schemes. It is unclear whether or not these phenomena are caused by the inherent magnetic structure and/or the inhomogeneous medium produced by the dipolle confinement system.

The purpose of the present work is to understand the density limit in a dipole plasma confinement (due to overdense heating, thermal particle transport, *etc*.). As a first approach, we studied the propagation and absorption of electromagnetic waves numerically for the inhomogeneous region of a dipole plasma confinement system that contains a self-organized plasma.

2. Propagation and Absorption of EM Waves in an Inhomogeneous Medium

Figure 1 shows the EC heating system and main diagnostics of the RT-1 device. The inside of the vacuum vessel is evacuated to 10^{-6} Pa. The working gas (hydrogen or helium) is introduced into the vacuum vessel up to a range of more than 10^{-4} Pa, and we then use electron cyclotron resonance heating (ECRH) to produce and sustain the plasmas.

For the ECRH, we introduce an EM wave from an 8.2 GHz klystron (Toshiba, nominal power 100 kW) into the vacuum vessel through the transmission lines L#1 and #2 (up to 25 kW/line). The EM wave is launched from the upper ports obliquely toward the fundamental ECR

author's e-mail: mori.takahiro18@ae.k.u-tokyo.ac.jp
*) This article is based on the presentation at the 27th International Toki Conference (ITC27) & the 13th Asia Pacific Plasma Theory Conference (APPTC2018).

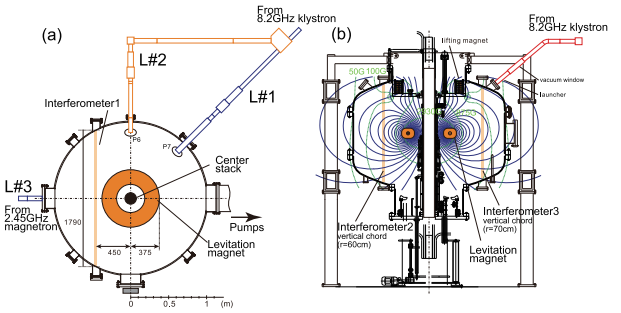

Fig. 1 (a) The equatorial plane, and (b)a poloidal cross-section of the RT-1 device. The transmission lines L#1 and L#2 are used for 8.2 GHz EC heating and L#3 is used at 2.45 GHz.

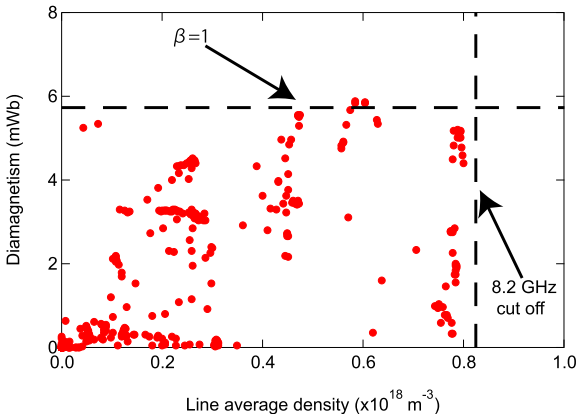

Fig. 2 Density limit observed in the RT-1 for 8.2 GHz ECH, where the working gas is hydrogen or helium.

layer, which lies across the levitated magnet. The EM wave propagates via the edge region of the plasma to access the absorption layer. In the RT-1 experiment, we measured the line integrated density using interferometer 1 (IF 1). We determined the 1.6 m chord length of IF 1 from the two points at which the last closed flux surface crosses the chord. The line integrated density divided by the chord length gives the line averaged density. To determine the density limit for 8.2 GHz ECH, we varied the injected power from 0 to 40 kW. The pressure of the hydrogen fill gas ranged from 1 mPa to 80 mPa and for helium from 3 mPa to 28 mPa. For 8.2 GHz ECH, the electron density limit is 8.0×10^{17} m^{-3} [2], as shown in Fig. 2. According to the results of the interferometric density reconstruction, the core density reached a so-called over-dense state. We also introduced an EM wave from a 2.45 GHz magnetron (nominal power 20 kW) into the vacuum vessel from the equatorial port through transmission line L#3. The EM wave propagates perpendicular to the magnetic fields. In this case, the fundamental ECR layer lies across the plasma in the confinement region, and the EM wave has to cross the peak-density region to reach the ECR layer.

To simulate the propagation of the EM waves, we start from Maxwell equations:

$$\nabla \times \boldsymbol{B} = \frac{1}{c}\frac{\partial \boldsymbol{D}}{\partial t}, \tag{1}$$

$$\nabla \times \boldsymbol{E} = -\frac{1}{c}\frac{\partial \boldsymbol{B}}{\partial t}, \tag{2}$$

where $\boldsymbol{B}$ is the magnetic flux density, $\boldsymbol{D} = \boldsymbol{\epsilon} \cdot \boldsymbol{E}$ is the electric flux density and c is the speed of light. After Fourier transforming Eqs. (1) and (2) in time and space, we combine them to obtain the homogeneous-plasma wave equation with $\mathbf{n} = \frac{kc}{\omega}$.

$$\mathbf{n} \times (\mathbf{n} \times \boldsymbol{E}) + \boldsymbol{\epsilon} \cdot \boldsymbol{E} = 0. \tag{3}$$

Here, ω is the angular frequency and $\boldsymbol{k}$ is the wavenumber vector. The cold-plasma dielectric tensor is given by [3].

$$\boldsymbol{\epsilon} \cdot \boldsymbol{E} = \begin{pmatrix} S & -iD & 0 \\ iD & S & 0 \\ 0 & 0 & P \end{pmatrix} \begin{pmatrix} E_x \\ E_y \\ E_z \end{pmatrix}. \tag{4}$$

where

$$S = \frac{1}{2}(R + L), D = \frac{1}{2}(R - L),$$

$$R \equiv 1 - \sum_s \frac{\omega_{ps}^2}{\omega\,(\omega + \Omega_s)},$$

$$L \equiv 1 - \sum_s \frac{\omega_{ps}^2}{\omega\,(\omega - \Omega_s)},$$

$$P \equiv 1 - \sum_s \frac{\omega_{ps}^2}{\omega^2},$$

$$\omega_{ps}^2 \equiv \frac{4\pi n_s q_s^2}{m_s}, \Omega_s = \omega_{cs} \equiv \frac{q_s B}{m_s c}.$$

m_s is the and n_s is the number density of particles of species s with charge q_s, and $\Omega_s = \omega_{cs}$ is the cyclotron or gyrofrequency for particles of type s.

We have simulated the propagation of 2.45 GHz and 8.2 GHz EM waves in plasmas using a finite element method, full-wave calculation with COMSOL software. The specific solver we used is the direct solver MUMPS. The EC waves for 8.2 GHz are injected from the diagonal port and the 2.45 GHz waves from the horizontal port. The mesh size is less than or equal to one twentieth of the wavelength (0.6 ~ 6 mm at 2.45 GHz, 0.18 ~ 1.8 mm at 8.2 GHz). The center stack is defined to be an absorption boundary, and the other boundaries are treated as perfect electrical conductors.

Figure 3 (a) shows the magnetic field lines produced by the superconducting ring magnet (115 A, 2160 turns) and the levitation magnet (430 A, 68 turns). We assumed the electron density profile given by Eq. (5) and shown in Fig. 3 (b):

$$n_e(r,z) = n_0 \times \exp\left(-a\left(\frac{\psi(r,z) - \psi(r_{max},0)}{\psi(1,0)}\right)^2 \left(\frac{B(r,z)}{B_0(r,z)}\right)^{-b}\right). \tag{5}$$

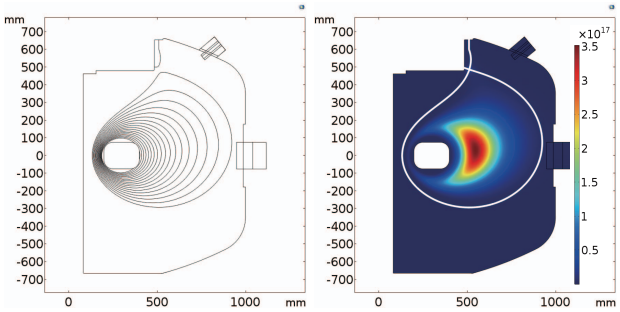

(a) Magnetic flux surfaces (b) Electron density $n_e(\mathrm{m}^{-3})$

Fig. 3 (a) Magnetic flux surfaces and (b) electron density profile to calculate the propagation of an EM wave in plasmas.

Here, $B(r,z)$ is the magnetic field at position (r,z), $B_0(r,z)$ is the magnetic field at $(z=0)$ which is on the flux fanction ψ at (r,z). The quantities (r_0, a, b, r_{max}) are fitting parameters. The fitting parameters are determined as the peak density $n_0 = 3.5 \times 10^{17}\,\mathrm{m}^{-3}$, other parameters are $a = 9.33, b = 1.084, r_{max} = 0.547\,\mathrm{m}$ by the results from interferometer 1, 2, and 3. The white line in the figure shows the separatrix.

3. Simulation Results

3.1 Density dependence

We investigated the experimental density limit for 2.45 GHz ECH, with the result shown in Fig. 4. For 2.45 GHz ECH, we varied the injection power from 0 to 18 kW. The gas pressure of the helium fill ranged from 0.28 mPa to 3.2 mPa. The density limit appeared at $\overline{n_e} = 1.6 \times 10^{17}\,\mathrm{m}^{-3}$, which exceeds the cutoff density for 2.45 GHz. Compared with the case for 8.2 GHz ECH in Fig. 2, there is a substantial difference between the cutoff density and the density limit for 2.45 GHz ECH. For the line averaged density of $\overline{n_e} = 1.6 \times 10^{17}\,\mathrm{m}^{-3}$, the peak density was $n_0 = 3.5 \times 10^{17}\,\mathrm{m}^{-3}$. In the following simulation, we changed n_0 while keeping the other profile parameters the same.

The EM wave propagates and reflects at $R = 0$ for the X-mode or at $P = 0$ for the O-mode, as shown in Figs. 5 (a) and 5 (b). When an EC wave is launched from the equatorial port, the propagation and reflection for both the O- and X-modes is similar because the $P = 0$ layer is close to that for $R = 0$. The vacuum vessel also influences the reflected EM waves.

We simulated the dependence on the electron density for three typical cases :below, equal to, and above the cutoff density. The results are shown in Fig. 6. The 2.45 GHz EM wave can reach the ECR layer directly when $n_0 = 3.5 \times 10^{16}\,\mathrm{m}^{-3}$, as shown in Fig. 6 (a). When n_0 exceeds $7.0 \times 10^{16}\,\mathrm{m}^{-3}$, the EM wave is divided into two paths by the cutoff layer, which makes it difficult for the EM wave to reach ECR layer. However, multiple reflections from the vacuum vessel and the three dimensional

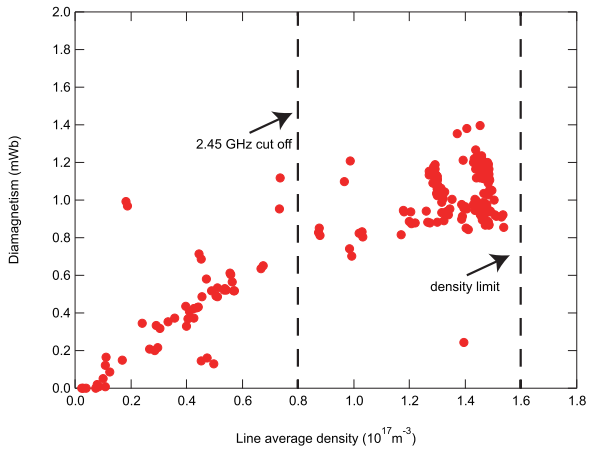

Fig. 4 Density limit observed in the RT-1 at 2.45 GHz ECH. The working gas is helium.

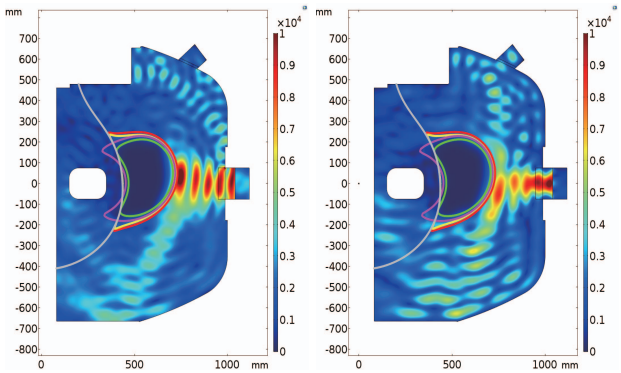

(a) O-mode excitation (b) X-mode excitation

Fig. 5 2.45 GHz EM wave propagation when the plasma density is close to the limit shown in Fig. 4. The red line is $R = 0$, the pink line is $P = 0$, the green line is $L = 0$, the yellow line is $S = 0$ and the gray line is ECR layer.

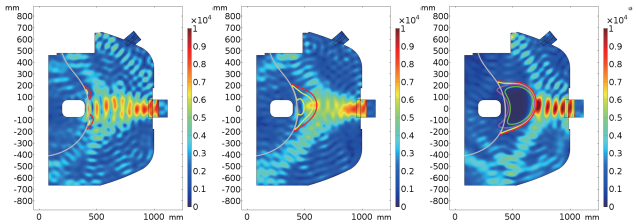

(a) (b) (c)

Fig. 6 Propagation of 2.45 GHz O mode EM wave. (a) $n_0 = 3.5 \times 10^{16}\,\mathrm{m}^{-3}$, (b) $n_0 = 7.0 \times 10^{16}\,\mathrm{m}^{-3}$, (c) $n_0 = 2.5 \times 10^{17}\,\mathrm{m}^{-3}$.

geometory actually make this possible.

3.2 Power absorption of EM waves for 2.45 GHz

We calculated the wave propagation based on the cold plasma approximation introduced in the previous section. We used these calculated wave propagation is re-

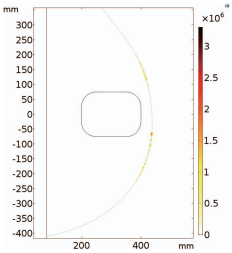

Fig. 7 The spatial profile of power absorption from a 2.45 GHz EM wave, in units of W/m^3, when $n_0 = 3.5 \times 10^{16}$ m^{-3}.

sults to evaluate the absorption of the EM waves at the resonance point. According to the hot-plasma model, the power absorption per unit volume in a plasma is given by Eq. (6) [4, 5].

$$P_{abs} = \frac{\omega_{pe}^2}{2k_z v_{Te}} \sqrt{\frac{\pi}{2}} \exp\left(-\frac{(\omega - \omega_{ce})^2}{2k_z^2 v_{Te}^2}\right) \frac{\epsilon_0}{2} \left|E_x - iE_y\right|^2 . \tag{6}$$

Here, ω_{pe} is the electron plasma frequency, and $v_{Te} = \sqrt{2k_B T_e/m_e}$ is the electron thermal velocity, where k_B is Boltzmann's constant. The z-direction is parallel to the magnetic field, and $\boldsymbol{k}$ is the wavenumber vector, which is parallel to the angle of incidence of the EM waves, and k_z is the z-component of that vector. The quantities E_x and E_y are the x- and y-components of the wave electric field. We calculated the local values P_{abs} on the mesh points, and we obtained the total power absorbed P_{abs}^{total} by integrating over the entire calculation space. The efficiency of power absorption is defined as the ratio of P_{abs}^{total} to P_{in}, where P_{in} is the incident EM wave energy. We calculated the profile of the power absorption using $n_0 = 3.5 \times 10^{16}$ m^{-3}, assuming a spatially uniform electron temperature T_e =10 eV. As shown in Fig. 7, the absorption concides with the fundamental ECR layer. (In this case, we ignored the absorption of the second harmonics.) The efficiency of power absorption reaches a maximum value of $\sim$ 70% at $n_0 = 2.5 \times 10^{16}$ m^{-3}, and it vanishes at $n_0 = 4.2 \times 10^{16}$ m^{-3}, as shown in Fig. 8, even though the EM wave reaches the ECR layer.

3.3 Power absorption from 8.2 GHz EM waves

We also simulated the propagation of 8.2 GHz EC waves in the RT-1 device. Figure 9 shows three cases of propagating 8.2 GHz EM waves. When $n_0 = 3.5 \times 10^{17}$ m^{-3}, the 8.2 GHz EM wave reaches the ECR layer. For $n_0 > 1.0 \times 10^{18}$ m^{-3}, however, the EM wave is interrupted by the cutoff layer before reaching the ECR layer, as shown in Fig. 9 (b). When $n_0 = 1.0 \times 10^{19}$ m^{-3}, the cutoff layer moves toward the outer wall of thevessel, and the EM wave does not reach the ECR layer, as shown in Fig. 9 (c). The ECR layer attains a power absorption per unit volume of $\sim$ 1MW/m^3 for both 2.45 and 8.2 GHz EM waves.

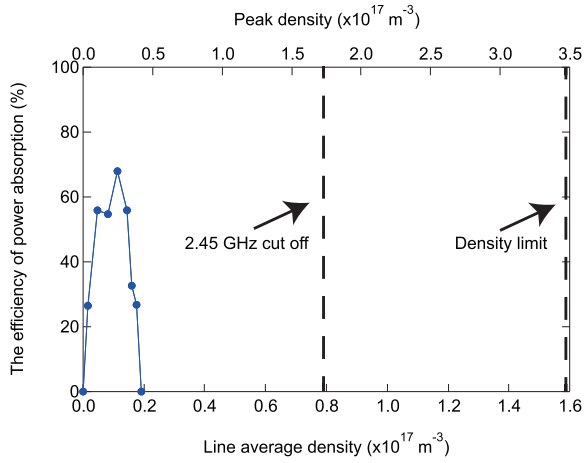

Fig. 8 The absorption efficiency of 2.45 GHz O-mode EM wave as a function of the line averaged density for T_e = 10 eV.

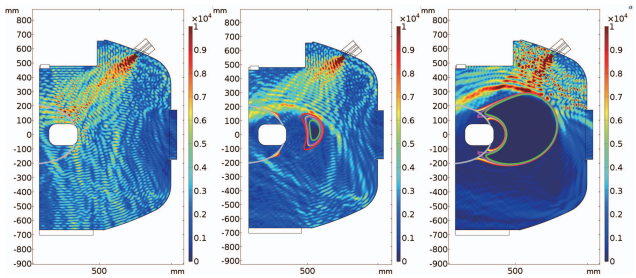

Fig. 9 The propagation of 8.2 GHz, X-mode EM waves for (a) $n_0 = 3.5 \times 10^{17}$ m^{-3}, (b) $n_0 = 1.0 \times 10^{18}$ m^{-3}, (c) $n_0 = 1.0 \times 10^{19}$ m^{-3}.

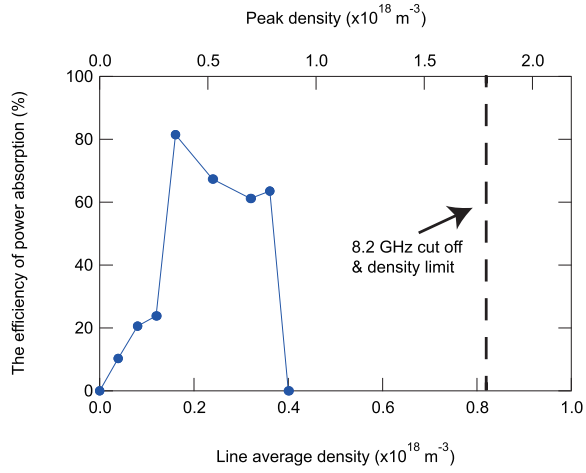

Fig. 10 The absorption efficiency of an 8.2 GHz X-mode EM wave as a function of the line averaged density with T_e = 10 keV.

The efficiency of power absorption drops to zero at $n_0 = 9.0 \times 10^{17}$ m^{-3}, which is close to the cutoff density for 8.2 GHz which is also the density limit, as shown in Fig. 10. To produce over-dense plasma at 8.2 GHz, we

must therefore propose another method of introducing the EM wave.

4. Discussion

In order to clarify the limitations of our present modeling efforts, we discuss here the simplifications and/or assumptions we used in the present model that should be improved in future studies. This discussions is intended to fill the gaps between the experiments and the simulations.

We calculated two-dimensional EM wave propagation in order to understand the density limits observed in the RT-1 magnetospheric plasma experiments. We reduced the spatial dimensions from three to two. Thus, we are unable to calculate the spread of the propagating waves in the toroidal direction. Waves hitting a wall are scattered partially into the same plane but mostly away in the toroidal direction. Therefore, our model treats the boundary at the center wall as an absorbing boundary, while the other, surrounding, walls are assumed to be perfect electrical conductors. Multiple reflections from the stainless-steel wall surfaces severely influence the distribution of the wave, which affects the quantitative analysis. Thus, it is possible that effects not included in this calculation may cause at least some disagreement between the simulations ans the experiments.

An Electron Bernstein Wave (EBW) is a longitudinally polarized electrostatic mode that propagates nearly perpendicular to the magnetic field. To excite an EBW, mode conversion from electromagnetic to electrostatic must occur in the plasma [6, 7]. For example, the X-mode wave can access to an upper-hybrid resonance layer where it can be converted into an EBW. Three scenarios for exciting EBWs are well known [8].

1. Perpendicular injection of X-waves from the high-field side (slow X-mode - EBW (SX-B) conversion)
2. Perpendicular injection of X-waves from the low-field side (fast X-mode - EBW (FX-B) conversion)
3. Oblique injection of O waves from the low-field side (O-mode - slow X-mode -EBW (O-X-B) conversion)

Our experiments achieved a density exceededing the cutoff density, but we have not yet investigated EBW heating or other effects mentioned above for the case in which we used the 2.45 GHz X-mode injection from the equatorial port. Further studies are thus required to understand the result shown in Fig. 8.

The power absorption in our simulation is not a self-consistent solution, because we solved the propagation of the EM waves and the power absorption independently. In addition, Eq. (6) for the power absorption is calculated from the second approximation for the hot-plasma dielectric tensor.

The locations of the ECR layers are different for 2.45 GHz and 8.2 GHz. The 8.2 GHz ECR layer lies across the levitated superconducting magnet. From the viewpoint of electron heating, this situation is disadvantageous compared with 2.45 GHz-ECH. However, the density limit occurs at 8.0×10^{17} m^{-3} for the 8.2 GHz-ECH. The actual density limitachieved is still higher than that at 1.6×10^{17}m^{-3} for the 2.45 GHz-ECH, and it is dominated by the cutoff density rather than by the location of the ECR layer. The over-dense state we observed for 2.45 GHz-ECH cannot be explained by the heating location, because the absorption efficiency at both frequencies is as high as 60 - 70%.

5. Conclusion

We have studied the propagation of EM waves in plasmas generated in the RT-1 device both through experiments and through full-wave simulations of the production and heating of a magnetospheric plasma. We solved the propagation ofthe EM waves using the cold plasma approximation, and we evaluated the power absorption. Density limits occured in the magnetospheric plasma experiments for both 8.2 GHz and 2.45 GHz ECH. The actual density limits observed in the experiments exceeded the cutoff densities at both frequencies. The simulated EM waves are absorbed below the cutoff densities at both frequencies, because the density is inhomogeneous and its gradient deflects the EM waves. The present simulation cannot explain the experimentally observed over-dense states and density limits in the view of the power absorption. The discrepancy may be due to multiple reflections of the EM waves, which makes the ECR layer accessible from the high-field side. Another possibilitiy may be mode conversion to an EBW [8]. In a dipole plasma confinement, the peak of the density profile exceeds the cutoff density at both frequencies. This feature may also indicate the generation of self-organized plasmas with up-hill diffusion [1]. Further study is thus needed to understand the density limits in the magnetospheric plasmas produced in the RT-1 device.

Acknowledgments

Authors would like to thank Dr. H. Saitoh of the University of Tokyo for discussion. This work was supported by the NIFS Collaboration research program (NIFS15KOAH034, NIFS19KBAR026), and JSPS KAKENHI Grant No. 17H01177.

[1] Z. Yoshida *et al.*, Phys. Plasmas **17**, 112507 (2010).
[2] M. Nishiura *et al.*, Nucl. Fusion **55**, 053019 (2015).
[3] T.H. Stix, *Waves in Plasmas* (AIP press, 1992).
[4] K. Miyamoto, *Plasma Physics for Controlled Fusion* (Iwanami Book, 2012).
[5] I. Fidone *et al.*, Phys. Fluids **21**, 645 (1978).
[6] H.P. Laqua *et al.*, Phys. Rev. Lett. **78**, 3467 (1997).
[7] R. Ikeda *et al.*, Contrib. Plasma Phys. **50**, 567 (2010).
[8] K. Uchijima *et al.*, Plasma Fusion Res. **6**, 2401122 (2011).